Int Surg 2018;**103:**493–504
DOI: 10.9738/INTSURG-D-16-00236.1

Comparative Analysis for Internal Fixations of Pauwels II by Biomechanical Finite Element Method

Matthew Jian-Qiao Peng[1], Xiangyang Ju[2], Hai-Yan Chen[3], Bai Bo[1], XinXu Li[4]

[1]*Orthopedics Department of 1st Affiliated Hospital, Guangzhou Medical University, China*

[2]*Department of Clinical Physics and Bioengineering, University of Glasgow, UK*

[3]*Orthopedics Department, HuiDong People's Hospital, HuiZhou, China*

[4]*Traumatic Orthopedics Department, SanShui People's Hospital, China*

Purpose: A series models of surgical internal fixation for femoral neck fracture of Pauwels II will be constructed by an innovative approach of finite element so as to determine the most stable fixation by comparison of their biomechanical performance.

Method: Seventeen specimens of proximal femurs scanned by computed tomography in Digital Imaging and Communications in Medicine (DICOM) format were input onto Mimics rebuilding 3D models; their stereolithography (STL) format dataset were imported into Geomagic Studio (3D Systems, Rock Hill, South Carolina) for simulative osteotomy and non-uniform rational basis spline kartograph; the generated IGS dataset were interacted by UG to fit simulative 3D-solid models; 3 sorts of internal fixators were expressed in 3D model by ProE (PTC, Boston, Connecticut) program virtually. Processed by HyperMesh (Altair, Troy, Michigan), all compartments (fracture model + internal immobilization) were assembled onto 3 systems actually as: Dynamic hip screw (DHS) / Lag screw (LS) / DHS+LS. Eventually, a numerical model of finite elemental analysis was exported to ANSYS for solution.

Result: Three models of internal fixations for femoral neck fracture of Pauwels II were established and validated effectively, the stress and displacement of each internal pin were analyzed, the advantages of each surgical therapy for femoral neck fracture of Pauwels II were compared and demonstrated synthetically as: "The contact stress of 3-LS-system was

Corresponding author: Bai Bo, Orthopedics dept. of 1st Affiliated Hospital, Guangzhou Medical University, 151 Yan Jiang Xi Rd., Guangzhou, China 510120.
Tel.: +86 20 8306 2680; E-mail: 18922346634@163.com

checked to be the least; the interfragmentary displacement of DHS+1-LS assemblages was assessed to be the least."

Conclusion: 3-LS-system is recommended to be a clinical optimization for Pauwels II femoral neck facture, by this therapeutic fixation mechanically, breakage of fixators, or secondary fracture rarely occurs.

Key words: Pauwels II fracture – Internal fixation – Finite element analysis – Biomechanics method – Contact stress

Vertical femoral neck fracture is a problematic orthopedic injury due to the domination of indirective shear forces caused by high-energy trauma through mechanotransduction. Of the total hip fractures facing old men greater than 75 years old, the ratio of femoral neck facture is about 50%~60%[1]. There are existing options such as internal fixation, full hip replacement, or half hip replacement without a standard for treatment clinically. Many factors must be considered, including fracture type or bone quality problem such as osteoporosis. A hypothesis that 3-LS-Fixation is a preferred therapeutic technique by surgeons is likely because of less susceptibility to screw breakage or secondary fracture;[2] however, little is known about why and how biomechanics govern this assumption now. The mathematical model is novel for augmenting experimental analysis by providing information about potential regulatory mechanisms for treatment. Biomechanical examination is a cornerstone for development of surgical implants in fracture stabilization as failure to stabilize results in reoperation. It is important to determine optimal fixator prior to surgery to reduce the likelihood of stress fractures as well as associated complications. The aim of this study is to compare the performance of 3 pinning methods namely dynamic hip screw (DHS), lag screw (LS), and DHS+LS for femoral neck fractures to address clinical confusion. Thus, this paper will numerically investigate all internal pins for Pauwels II (one of the Pauwels classifications oriented by fracture line toward horizontal line) of femoral neck facture by computerized model of finite element analysis (FEA) so as to find the most stable fixation method addressing clinical decision quantitatively.

Materials and Methods

This paper evaluated 17 sets of CT scanning from intact femur of healthy adult volunteers (with informed consent) without abnormalities or impairment of altering bone morphology, medical Image Materialis Mimics, reverse engineering software Geomagic Studio 12.0, interactive CAD/CAM software UG-8.0 (Siemens, Nurnberg, Germany), 3D drawing software ProE-5.0, pre-FEA processor HyperMesh 11.0, FEA software ANSYS 14.0 (ANSYS, Cannonsburg, Pennsylvania).

Femur model rebuilt

After 17 sets of images were scanned by CT, the generated data of Digital Imaging and Communications in Medicine (DICOM) format was numerically obtained and input onto Mimics software for manual 3D reconstruction manually.[3] The default bony gray value for Mimics is 226~2311, set to threshold value. This femur was separated by thresholding. The digitized sections of proximal femur were extracted by region growing, the Edit mask function on the Mask module was then executed to erasure, protract, and or calculate the 3D model. A proximal femur model of STL format is visualized.

Fracture model developed

The aforementioned 3D model of STL was imported to reverse engineering software Geomagic Studio 12.0, and then meshed by function of the Grid doctor. Its osteotomy was processed by the Plane section module modified to simulate fracture (transversely cutting femur at its mid-neck orientated at 50° with respect to horizontal plane) through a series of procedures called Probe curvature → Degraded contour → Construct surface patches → Construct grid → Fitting surface, etc. A NURBS kartograph was fitted to be femoral head, and then the femoral shaft is to be fitted similarly. They were all saved by *.IGS format.

Solid model fitted

The previously mentioned acquired kartograph models of femoral head and shaft were imported to commercially available interactive CAD/CAM software, namely UG-8.0, for further refining. An

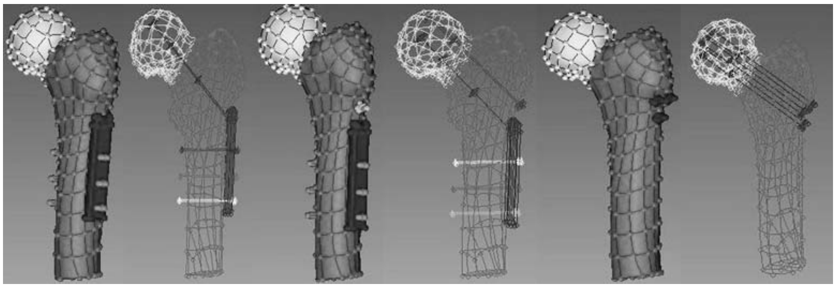

Fig. 1 Three systems of internal immobilization of fracture assembled. Left to right: DHS versus wire frames, DHS + LS versus wire frames, 3-LS versus wire frames.

entity model of solid is conversed by its functions of Insert → Combine → Fit by clicking the Checking GeometricSolid module by its Surface Sweeping Method to check the model until it accomplished.

Fixation model designed

According to the clinical size of AO / ASIF, 3 sorts of internal immobilization for fracture were designed in a 3D drawing program called Pro-Engineer (ProE-5.0). They are instrumentation systems of DHS, 3-LS, and DHS+1-LS. Screw thread is omitted here as it is not particularly relative to our study. Instead, it is substituted by the same diameter cylinder. The parameters of internal fixators are based on the reference[4] to construct this instrumented model.

FEA model created

Model assembled

The aforementioned femoral fracture model and internal fixation models are synthetized and imported onto pre-FEA software namely Hypermesh 11.0. There, tools of Translate and Rotate were executed to move and rotate the fixation model so that fixators (3 screws secured) are dispersed and perpendicular to the fracture line. The interfaces between screws and femur were simplified by assigning the contact surfaces to be bonded. These 3 screws must be parallel to make up a Trigono-carpus, so that the longitudinal axis of the femoral shaft joins the DHS at an angle of 135°; in the DHS+LS system, DHS must be parallel to LS. The integrated models in combined fracture/fixator constructs are installed geometrically as displayed by Fig 1.

Mesh plot

All these models are adopting tetrahedral 8-node elements of solid-185 volume element. All compartments are divided as a 2D grid and then upgraded to a 3D grid. They are meshed into remodel and saved as solution format of *.cdb for extraction after material property is assigned.

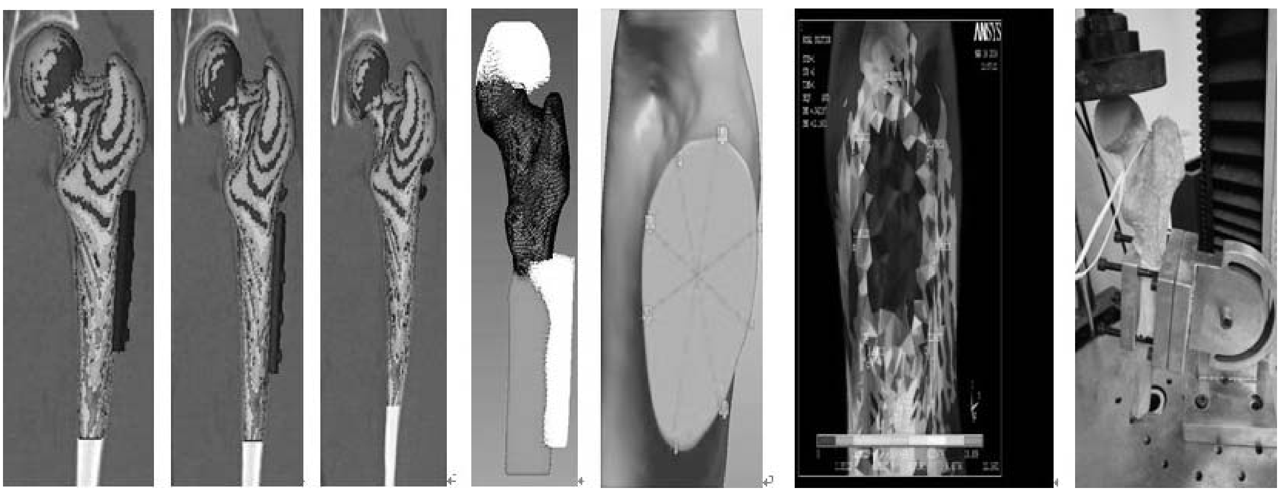

Fig. 2 The first three panels show FEM material assigned; left to right: DHS, DHS + LS, LS. The last four panels show verification of model validity; left to right: Constrain, Node plane, Model validity, Cadaveric validity.

Table 1 Stress values for each 8-node of 12 FE samples

	Position #							
Sample #	1	2	3	4	5	6	7	8
1	0.95962	1.08178	0.722216	0.222289	2.21429	1.231093	0.725866	0.600427
2	2.365501	0.522318	2.214457	0.290111	4.60191	2.907203	1.0395	0.713425
3	1.89497	1.204012	1.012684	0.467758	2.768523	2.102543	1.328077	0.819144
4	0.620409	0.399854	1.045387	0.371484	2.942854	2.261493	0.730747	0.462416
5	3.186124	1.094655	2.260299	0.609772	2.836237	2.868277	1.982035	0.202032
6	1.23152	2.22689	2.58363	0.754154	4.946323	2.627293	1.195486	0.950645
7	1.54106	1.06443	1.885397	0.354257	2.39623	1.369875	0.971287	0.798693
8	1.703297	0.650252	1.278543	0.205116	1.87754	1.337363	1.518337	1.046773
9	2.173445	1.507025	1.764093	0.862081	3.858323	3.472113	1.147653	0.367901
10	2.38251	0.916799	1.276729	0.970677	3.069833	2.331347	0.668171	0.883533
11	1.507317	0.710776	1.338166	0.412746	2.74588	1.366152	0.683243	0.581944
12	1.417896	0.720122	1.34875	0.19126	1.19263	1.19263	1.249671	0.896941
Average (MPa)	1.748639	1.008243	1.560863	0.475975	2.954214	2.088949	1.103339	0.693656

Material assignment

The aforementioned dataset of *.cdb is returned to Mimics for material assignment. Five materials are assigned based on CT grayscale for bone as revealed by Fig 2.1. The material properties of the models are assumed to be linear elastic, isotropic, and homogeneous, according to the experience[5–7] of materials assigned (such as: Density = 1017 × Grayvalu — 13.4, E-Modulus = 5925 × Density — 388.8; Density = 1.067 × HU + 131, E-Modulus = 0.004 × density ^ 2.01) and data reported by published references[8–10] retrospectively. The bony modulus of elasticity is assigned, Poisson's ratio of femur is assumed to be 0.3; modulus of elasticity for screw fastener is set to be 190,000, while Poisson's ratio of it is 0.27; modulus of elasticity for steel screen is set to be 110,000, and Poisson's ratio of it is applied as 0.33. Since the focus of this study is to compare the performance of 3 fracture pin methods, this choice of isotropic material properties for bone is acceptable for modeling human femoral bone.

Contact boundary setting

The aforementioned model with property assigned was re-imported onto Hypermesh as to set Contact surfaces. All contacts between the two fracture fragments and the fixation are considered to capture the stresses and strains at the interface of the bone and fixator. The interfragmentary boundary condition and contact relationship is set under the menu of Contact Manager. Its frictional coefficient is set at f = 0.2[11] between implant-bone, and zero for pairing bone-bone, the contact unit is targe 170 / conta 174. The bone-screw interfaces in all cases are assumed to be fixed so as to increase the stability of numerical analyses and reduce the computational time.

Load configuration and constraint conditions

An adult weighted 70 kg standing by single foot erectly is simulated to stress feature of screw fixation. A compressive preload of 600N is applied via vertical imposing upon the bone structures and fixations, which is calculated by subtracting the weight of 1 leg from the body weight. The degree of freedom on a node basis of XYZ direction is constrained to be 0 for distal femur. That means the displacement in Cartesian coordinate system. The options for solution is defined finally. This FEM is exported by *.cdb format.

FEM solution

This generated FEM is to be imported onto ANSYS 14.0 for solution of computation and analysis. The observation index includes (1) Von Mises stress / displacement contours of femoral head / femoral shaft / fixator, and (2) Von Mises stress / displacement contours of the general model. The peak and distribution yield will be measured by then. Here the physiologic forces of ligament and muscle are not taken into account for these subjected models.

Validation for effectiveness of approach

There are 2 ways to validate the effectiveness of a FEM. One way is to compare the present method with previous researches of similar stress and displacement. By this way, our testing outcome is consent to the validating technique and retrieval

Table 2 Stress values for each 8-node of cadaveric femur

Node #	Strain #1	Strain #2	Strain #3	Strain average	Absolute value	Stress (MPa)
1	250	290	315	285	285	2.0805
2	−110	−120		−115	115	0.8395
3	−325	−350		−337.5	337.5	2.46375
4	−35	−35	−35	−35	35	0.2555
5	425	455	460	446.6667	446.7	3.26091
6	380	385		382.5	382.5	2.79225
7	190	185		187.5	187.5	1.36875
8	−30	−30	−30	−30	30	0.219

literature conducted by Zhang *et al*.[12] Another way is to develop a cadaveric model that resembles FEM *in vitro*. Validity will be verified by comparing the similarity of results for each experiment based on equal status:

It is assumed that FE model of the femoral neck is resected by a plane horizontally, and the circumference is intercrossed by 4 lines at 45° angles forming 8 nodes positioned as Fig 2 ($8 \times 45° = 360°$). When 600N is vertically pressed upon each of the correspondent 8 nodes of 12 samples revealed by Fig 2, their average values of stresses are presented as Table 1. On the other hand, strain foils were placed at relative positions of a cadaveric femur corresponding to FE model and linked to a Biomaterial Universal Testing Machine. Its load-strain curve was observed to record strain value when maximal pressure of 600N was reached. Force values are calculated to form Table 2 by formulas: Actual-strain = 10 × Measured-strain — 6 , Stress = Actual-strain × Elastic-modulus (here 7300MPa is chosen by reference[13]). These 2 tables are summarized as Table 3 and then visualized by Fig 3. That $P > 0.05$ from Independent Sample T Test indicates nothing significantly different between models of FE and cadaver. They are agreeable to each other, and our applied approach is reliably validated.

Result

Observation of stress

Stress of femoral head

As depicted by Fig 4, the contact stress of all femoral-head models are concentrated around fracture line (inferior to femoral neck or interface of fixation). Femoral head stress is actually pressure upon the fracture side. Generally, pressure is helpful to fracture healing. The rank-sum test of Kruskal-Wallis is designed and carried statistically by SPSS 13, by comparison among these 3 models one by one. P value is found to be 0.159, which is greater than 0.05, suggesting that there is no difference in significance among a (DHS) / b(DHS+LS) / c(LS) in terms of stress.

Stress of femoral shaft

By reviewing the following Von Mises and Histogram variation of Fig 5, the reaction stress of femoral shaft is assessed to distribute in equality. Most of the stress peaks disperse around the interface between fixator (screw) and fracture plane, between fixator and superior femoral shaft, and near lesser-trochanter inferior to femoral neck. Rank-sum of Kruskal-Wallis is examined statistically by SPSS 13 for stress peak. $P = 0.004 < 0.05$ suggests significant difference. By comparison among these 3 models two by two with inspection level of $\alpha = 0.05 / 3 = 0.017$: model a(DHS) is not significantly different when it is compared with model b(DHS + LS) as $P > 0.017$; however, it is significantly different whatever a(DHS) compares to c(3LS) or b(DHS + LS) compares to c(3LS) due to $P < 0.017$ for each. The average value of femoral shaft stress for c(3LS) is the least among the 3 models. That means c(3-LS) is evaluated to be the best as its potential risk of secondary fracture is lower.

Table 3 Stress comparison on correspond positions of FE model to cadaveric femur

	Node #							
Sample #	1	2	3	4	5	6	7	8
FE model	1.7486	1.0082	1.5609	0.4760	2.9542	2.0889	1.1033	0.6937
Cadaver	2.0805	0.8395	2.4638	0.2555	3.2609	2.7923	1.3688	0.2190

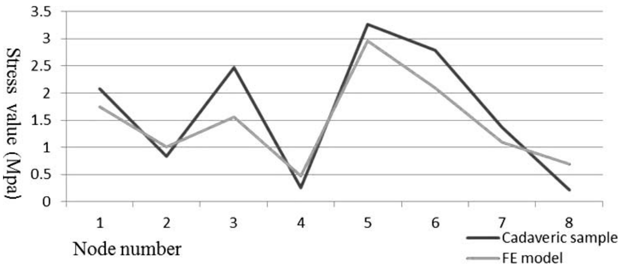

Fig. 3 Line chart for stress comparison between FE model and cadaveric femur.

Stress of internal fixator

The following Von Mises and Histogram in Fig 6 indicate the contact stress of Internal Fixator concentrates distribution. Its area focuses on the interface of facture and intermediate session of screw secured. It means the maximum shearing force is at the fracture section. $P = 0.001 < 0.05$ suggests the difference is significant when Kruskal-Wallis rank-sum is tested statistically for stress peak. By comparison among these 3 models two by two, we get all $P < 0.017$. The average value of Internal Fixator stress for a(DHS) is 196.97 Mpa, for b(DHS+LS) is 88.37 Mpa, and for c(LS) is 63.81 Mpa. The peak value of DHS is the greatest. This can be explained as: for a(DHS), the DHS screw is subjected by all compressive stresses; for b(DHS + LS), the stress peak decreases after 1 LS is added. A Trigonocarpus formed by 3 LS is able to discretize and or share stress of the whole assemblage and thus increase its stability. However, the more screws locked, the more bones destructed, so "the more screw the better therapy" is not reasonable.

Total stress of (fracture + fixator) integral system

By reviewing the following Von Mises and Histogram in Fig 7, we notice that because the elastic modulus for metal fixation is much greater than that of bone, peak stress lies on Internal Fixator, and distributes at the interface of fracture surface and screw due to concentrative principle of stress distribution. $P = 0.001 < 0.05$ suggests a significant difference while "Kruskal-Wallis Rank-Sum" is tested statistically addressing General stress. By comparison among these 3 models two by two, $P < 0.017$ is reached whatever a versus b, or a versus c, or b versus c. The average value of integral assemblage (Fracture + Internal Fixator) stress for a(DHS) is 195.35 Mpa, for b(DHS + LS) is 86.72 Mpa, and for c(LS) is 64.60 Mpa, the peak value of a(DHS) is the greatest, b(DHS+LS) is medium, and c(LS) is the least in sequence. Therefore, 3-LS instrumentation is the most stable immobilization of all models because its probability of screw breakage or secondary fracture is minimum and mechanical failure is avoidable.

Observation of displacement

Displacement distribution of femoral head

Vertical displacement of femoral head implies its ability of anti-inversion. The displacement along the fracture line of the femoral neck reflects its capability of anti-compression. By reviewing Fig. 8, we notice

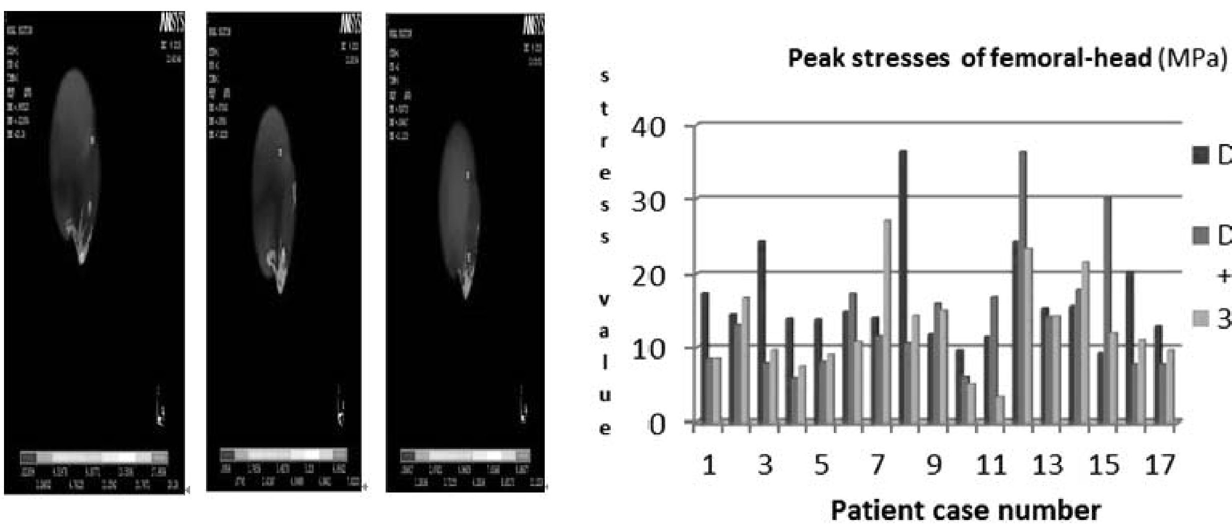

Fig. 4 Von Mises stress of femoral head (DHS, DHS + LS, LS) and histogram of femoral head stress.

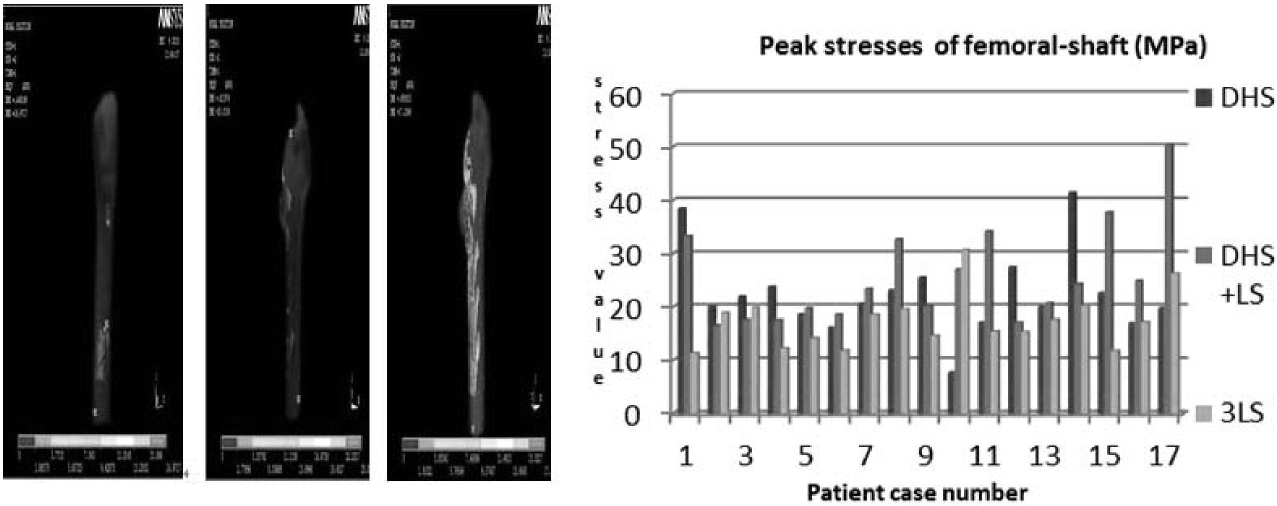

Fig. 5 Von Mises stress of femoral-shaft (DHS, DHS + LS, LS) and histogram of femoral shaft stress.

that the concentration region of peak displacement for femoral head is at the top directly, and gradually decreases inferolaterally concentric-circle like. The displacement directions of all femoral-head models are actually the resultant force lines, which are the vector sum of shear line and gravity line. It means both hip inversion or femoral neck compression may occur. $P = 0.016 < 0.05$ suggests a significant difference while Kruskal-Wallis rank-sum is examined statistically addressing displacement. By comparison among these 3 models two by two, $P > 0.017$ suggests no significant difference when a versus c; however, $P < 0.017$ suggests significant difference whatever a versus b or b versus c. The average value of a(DHS) is 1.068 mm, of b(DHS+LS) is 0.735 mm, and of c(3-LS) is 1.010 mm. Usually the less displacement is, the stapler a fixation is, or to speak in other words: b(DHS+LS) assemblage is stapler than other 2 assemblages.

Displacement distribution of femoral shaft

The displacement of femoral shaft implies its magnitude of fastness relative to Internal Fixator. By reviewing Fig. 9, we found that peak displacement of all models concentrate near greater-trochanter adjacent region, and decreases distally from concentric circles. Statistical information from the rank-sum test of Kruskal-Wallis is carried out by

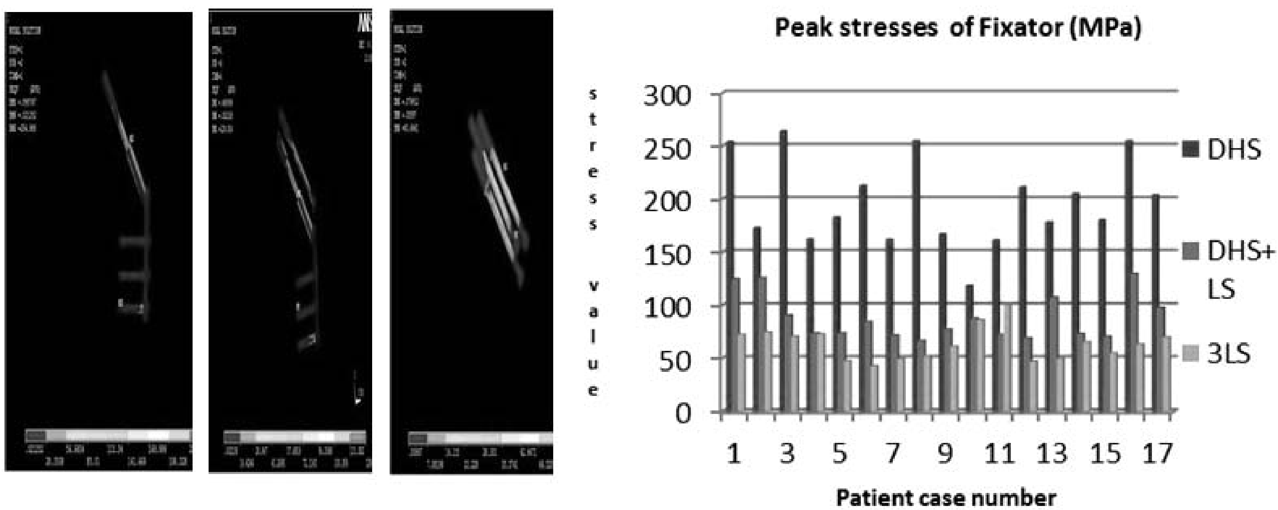

Fig. 6 Von Mises stress of internal fixator (DHS, DHS + LS, LS) and histogram of internal fixator stress.

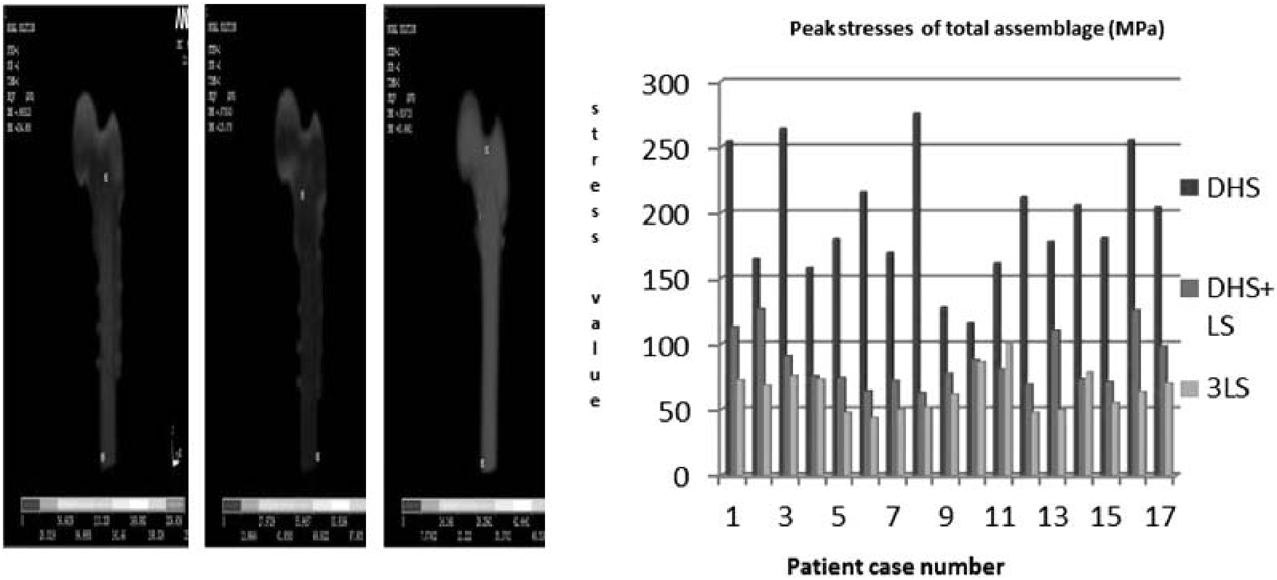

Fig. 7 Von Mises stress of total assemblage (DHS, DHS + LS, LS) and histogram of total assemblage

SPSS 13. $P = 0.029 < 0.05$ suggests a significant difference. Further comparison of either a versus b or a versus c reaches $P > 0.017$ suggests a difference that is not significant, but $P < 0.017$ for b versus c suggests a significant difference. The average value of femoral shaft displacement for a(DHS) is 0.533 mm, for b(DHS + LS) is 0.475 mm, and for c(LS) is 0.714 mm. The firmness of 3-LS assemblage is judged looser than others.

Displacement distribution of fixators

By reviewing Von Mises of fixators' displacement on Fig. 10, we found that the direction of fixator displacement is the same as that of femur, its peak values focus on screw-head inferior to femoral head, and gradually decreases by likelihood of concentric circles from screw head to screw tail. This displacement quantitatively reflects the magnitude of femur shortening or hip reversion. Statistical information from rank-sum test of Kruskal-Wallis is carried out by SPSS 13. $P = 0.020 < 0.05$ suggests a significant difference. Further comparison of either a versus b or b versus c reaches $P < 0.017$ suggests a significant difference, but $P > 0.017$ for a versus c suggests a difference that is not significant. The average value of pining displacement for a(DHS) is 0.973 mm, for

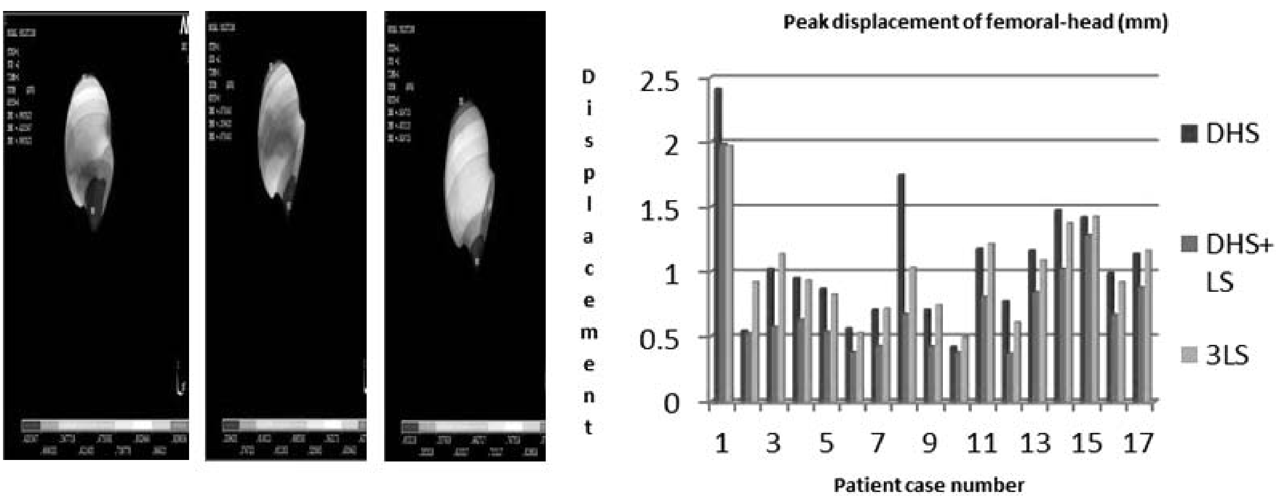

Fig. 8 Femoral head displacement Von Mises (DHS, DHS + LS, LS) and femoral head displacement histogram.

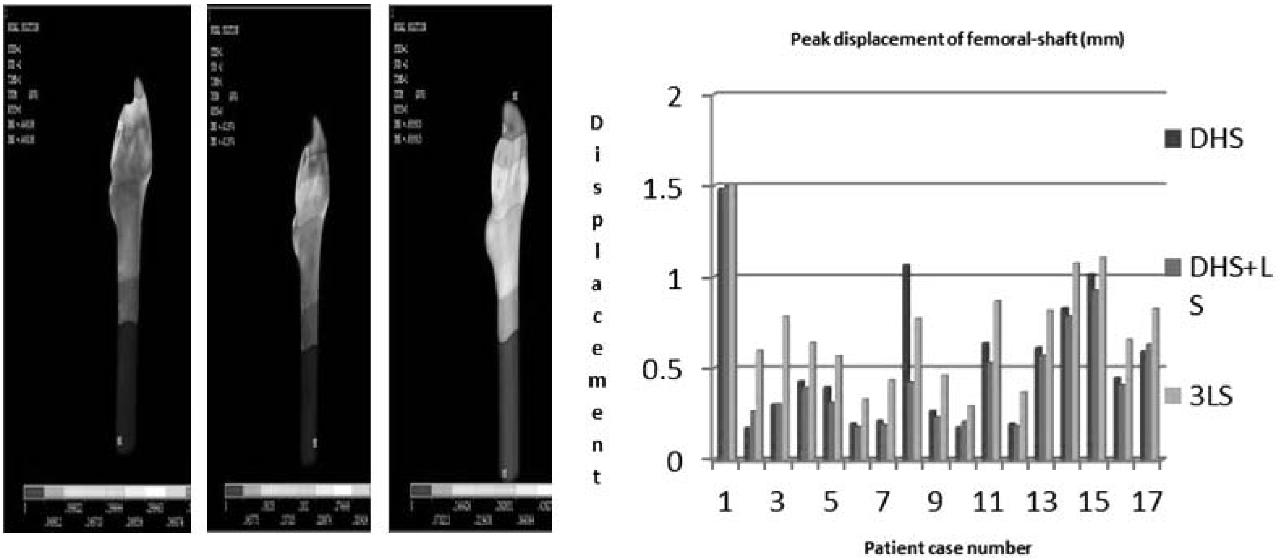

Fig. 9 Femoral shaft displacement Von Mises (DHS, DHS + LS, LS) and Femoral shaft displacement histogram.

b(DHS + LS) is 0.706 mm, and for c(LS) is 0.982 mm. The magnitude for anti-femur-shortening or anti-hip-reversion of assemblage b(DHS + LS) is judged greater than others.

Displacement distribution of integral (fracture + fixators) assemblage

By reviewing Von Mises of displacement on Fig. 11, we found that the directions of all fixators' displacements are the resultant force lines, which are actually the vector sum of shear line and gravity line. Their peak values are focus on femoral head subjected to force, and gradually decrease likely as a concentric circle toward fracture edge from stress position. The sense of displacement for integral (fracture + fixators) system is equivalent to that of femoral head, representing the ability of anti-inversion for fixator; the peak displacement for

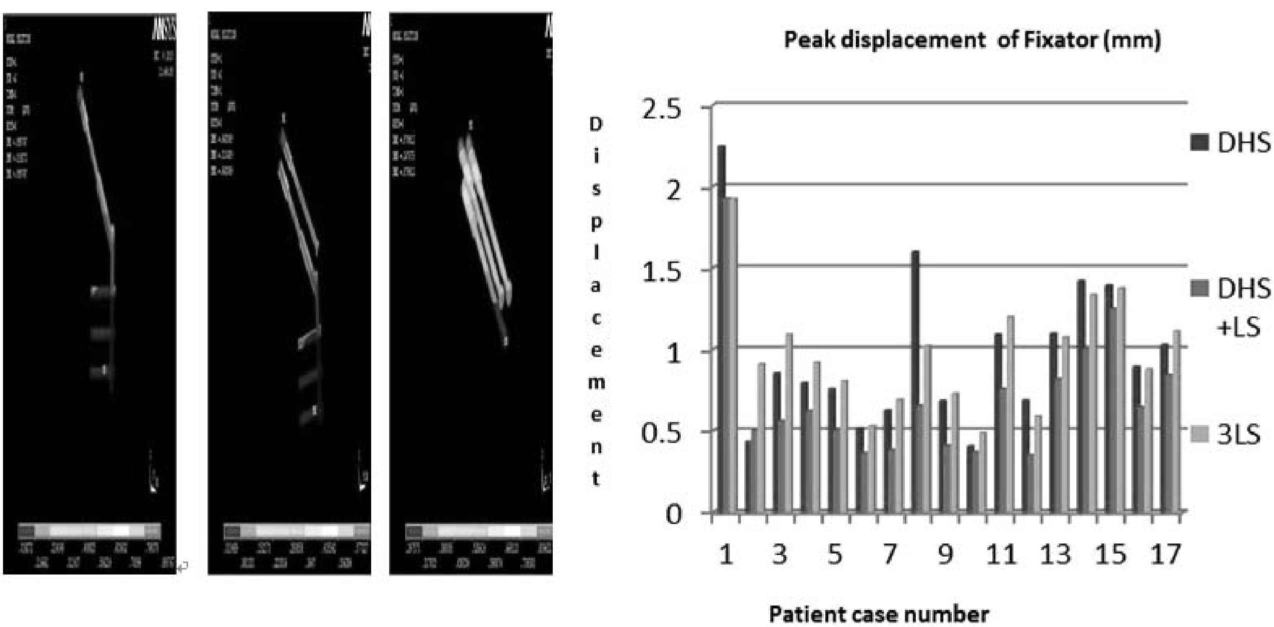

Fig. 10 Von Mises stress of fixator displacement (DHS, DHS + LS, LS) and histogram of fixator displacement.

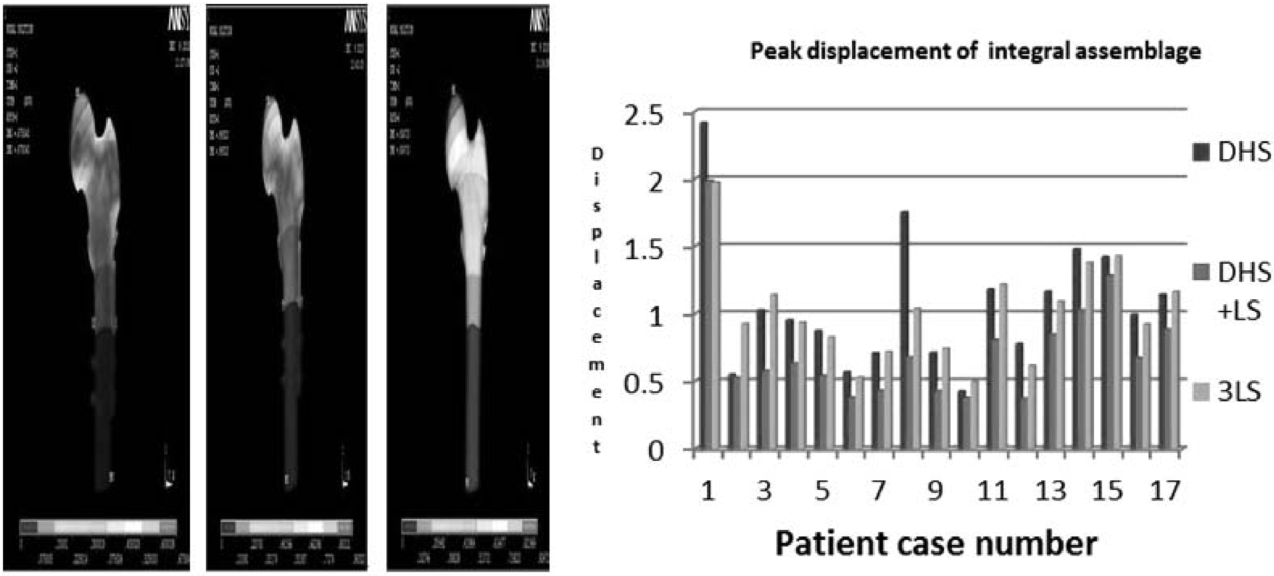

Fig. 11 Von Mises stress of integral assemblage displacement (DHS, DHS + LS, LS) and histogram of integral assemblage displacement.

general (fracture + fixators) assemblage is equivalent to that of femoral head; therefore, the mechanical stability of integral system is similar to that of femoral head.

Discussion

There are primarily 2 patterns to study biomechanics.[14] The first approach is Experimental Biomechanics, which tests mechanics by analyzing stress and strain addressing specimens of animal or cadaver and is difficult to handle complex engineering status. It is costly and unrepeatable although real model is probably established mechanically. Alternatively, the second algorithm is Theoretical Biomechanics.[15] Working by solution of computational model, its basic idea is to break up the whole into pieces and then combine these components into a whole, where cadavers could be replicated efficiently by artificial models. Purely experimental approaches are unable to fully describe biomechanism leading to fracture healing, whereas FE method geometrically enables evaluation of stress distribution and material properties, which are difficult to test experimentally. It is suitable for achieving parameters of determining more values than the experimental one. FEM solves clinical problems by predicting stress distribution throughout the structures of interest; Von Mises stress distribution along fracture line is then analyzed to identify location and magnitude of the maximal stress of each model. FEA examines biomechanical performance of implant designs and effect of clinical factors on implant by simulation, which enables researchers to predict and demonstrate influence of specific factors in a given system.[16] Our FEA is conducted to evaluate the pinning component based on comparison with 3 assemblages of internal immobilization to direct further optimization. Our model simulates physics solid by mathematical approximation and advances unlimited quantities from unknown quantities. Its validity and transferability realize soluble standard and perform accurate assessment of parameters on the likelihood of fracture to select optimal fixation for individuals. And apparently, its insight of computational finding will greatly improve the clinical decision process.

Minimally displaced fracture is usually managed with internal pinning to hasten rehabilitation. The constructs may fail consistently due to proximal fragment shifting or tilting a varus position. High rates of delayed nonunion occurs depends on multifactorial causes such as: bone structure, types of Pauwels, parallelism of fixation, pins positioning, alignment / gap after fracture reduction, as well as fracture line angle. CT-derived FEA of the femoral-pining not only predicts loads required and fracture locations but also indicates correlation of strain and displacement. Displacement is caused by traction, whereas fracture healing is accelerated by compression helpfully. Hooking fixation of increasing stress at fracture site probably results in nonunion, whereas stress on fracture line in Pauwels II consists of compression contributing to stabilization and promoting higher screw strength. From a clinical perspective, it is necessary to provide detailed information for planning of surgical resection or reorientation, identify respective outcomes of fracture repair, and suggest an optimal healing strategy of individuals. Computerized fracture pinning model is essential to address which sort of designated fixators matters most. Numerical investigations indicate that the DHS + LS method gets the lowest axial femoral head displacement and interfragmentary movement during static loading; it has the greatest resistance against shear and rotational forces because it keeps proximal and distal segments together more firm during the course of healing process.[17] Statistically, due to no significant difference of displacement between DHS + LS and 3-LS, which method is clinically suitable will depend on reaction stress analysis. DHS is subjected to higher stress because of smaller contact areas, which increase the wear rate, whereas maximum Von Mises stress decreases at the impingement location of 3-LS due to load distribute on larger surface. Reduction of load transfer by delaying weight-bearing is advantageous for fractures healing in fixation systems.[18] Our computational result of displacement indicates that DHS + LS and 3-LS pinning both offer the lowest femoral head displacement and interfragmentary movement, but 3-LS offers the strongest structure for stabilizing vertical femoral neck fracture. It is also consistent with clinical hypothesis that 3-LS-Fixation reduces stress at the femur-pins interface and increases biomechanical stability, and thus is accepted as surgical procedure for solid fixation of Pauwels II.

Although we developed FEA techniques in clinical practice by computational platforms to refine implant design and improve surgical operation with computerized procedure rehearsal, there are limitations remaining in this current study: the actual macroscopic property of cancellous bone (*i.e.*, linear isotropic and heterogeneous are both assumed for cortical and cancellous bone) is not taken into account, soft tissues such as joint capsule, ligaments, and periosteum are excluded from the analysis, so, whether our model can predict human bone fractures with the same degree of accurate description as the synthetic bones is unknown; caution is thus required when interpreting the data because FEA is only an approximation of the real situation, and the results should be evaluated by experimental and clinical data. Further investigation should be done in the future to reach a more precise conclusion.

Conclusion

This simulative study researched different therapies regarding Pauwels II fracture (femoral neck fracture with vertically oriented fracture line). The computerized model predicts incipient fracture pattern and resembles the actual pattern from the experiment. The most important aspect is the investigation of nonlinear stress analysis for fracture pins by 3D FEA, which is suitable for procuring biomechanical information to augment clinical surgery to minimize stress and improve fixation durability. Our experiment is built by innovative method of finite element distinctly. Its mechanics result is not only tested to be consistent with that of predecessors conducted previously but also passed validity exam, and is proven to be credible consequently.

Through detailed finite analysis, our most relevant finding, which is the novelty addressing clinical problem, is: this 3-LS-Fixation should be recommended as the first priority for therapeutic technique surgically as its peak stress is minimum, resulting in less susceptibility to screw breakage or secondary fracture. The stability of DHS-LS-Fixation is remarkably improved as its peak displacement is reduced comparable to that of 3-LS-Fixation. The potential risk of suffering from complications such as femoral neck compression or hip inversion becomes lower. It is, however, not significantly different from 3-LS Fixation. It is anticipated to be a practical procedure in case poor bone quality, such as osteoporosis, occurs. For DHS Fixation, there is no advantage to take whatsoever from stress or displacement; therefore, it is not considered clinically. This result enables operative planning in conjunction with computer-guided surgery to facilitate complex operation, whereby internal stresses and pressures are minimized.

Acknowledgments

Matthew Jian-Qiao Peng, MD, is a designer and writer. Xiangyang Ju, MD, handles mechanical analysis. Hai-Yan Chen, MD, is an experimental assistant. Bai Bo, MD, provides general instruction. Dr. XinXu Li, MD, performed clinical testing. No author associated with this paper has disclosed any potential or pertinent conflicts, which may be perceived to have impending conflict with this work. The statistical dataset and epidemiological methodology is included in the manuscript. All procedures performed in studies involving human participants were in accordance with the ethical standards of the institutional and/or national research committee and with the 1964 Declaration of Helsinki and its later amendments or comparable ethical standards. This work is supported by: Guangdong Department of Science Technology granted project (#2014A020215035); Guangzhou Medical University cultivation granted project (#2018z04); China Postgraduate Association granted project (B3-20170306-03); High Educational Research & Reformation Project 2018 and High Educational Postgraducate Innovation Plan 2018 (#2018JGXM79).

References

1. Moussa ME, Esposito CI, Elpers ME, Wright TM, Padgett DE. Hip dislocation increases roughness of oxidized zirconium femoral heads in total hip arthroplasty: an analysis of 59 retrievals. *J Arthroplasty* 2015;**30**(4):713–717.
2. Parker MJ, Khan RJ, Crawford J, Pryor GA. Hemiarthroplasty versus internal fixation for displaced intracapsular hip fractures in the elderly: a randomized trial of 455 patients. *J Bone Joint Surg Br* 2002;**84**(8):1150–1155.
3. Peng MJ, Hu Y, Ju X, Cai DZ. Clinical significance of creative 3D-image fusion across [CT + MR] modalities based on approach of characteristic co-registration. *J Med Imaging Health Inf* 2016;**6**(6):e71–e77.
4. Jin YP, Xu G, Wan QQ. Finite element analysis for firmness of 2 internal fixators of femoral neck fracture type Pauwels. *J ZheJiang Practical Medicine* 2010;**2**(2):123–126.
5. Hobatho MC, Rho JY, Ashman RB. Anatomical variation of human cancellous bone mechanical properties in vitro. *Stud Health Tech Inform* 1997;**40**(1):157–173.
6. Lan X, Liu X, Ge B. Debridement and bone grafting with internal fixation via anterior approach for treatment of cervicothoracic tuberculosis. *Int Surg* 2011;**96**(4):358–362.
7. Rho JY, Hobatho MC, Ashman RB. Relations of mechanical properties to density and CT numbers in human bone. *Med Eng Phys* 1995;**17**(5):347–355.
8. Sitthiseripratip K, Oosterwyck H V, Sloten J V, Mahaisavariya B, Bohez ELJ, Suwanprateeb J *et al*. Finite element study of trochanteric gamma nail for trochanteric fracture. *Med Eng Phys* 2003;**25**(2):99–106.
9. Kobayashi E, Wang TJ, Doi H, Yoneyama T, Hamanaka H. Mechanical properties and corrosion resistance of Ti-6Al-7Nb alloy dental castings. *J Mater Sci Mater Med* 1998;9(10):567–574.
10. Pioletti DP, Rakotomanana LR. Can the increase of bone mineral density following bisphosphonates treatments be explained by biomechanical considerations? *Clin Biomech* 2004;**19**(2):170–174.
11. Robinson PS, Placide R, Soslowsky LJ, Born CT. Mechanical strength of repairs of the hip piriformis tendon. *J Arthroplasty* 2004;**19**(2):204–210.
12. Zhang GD, Liao WJ, Tao SX. Exploration for material assignment and effectiveness validation of femoral neck FEA. *J Tissue Engineering Reach* 2009;**52**(3):10263–10268.
13. Gefen A, Megido-Ravid M, Jtzchak Y, Arcan M. Biomechanical analysis of the three-dimensional foot structure during gait: A basic tool for clinical applications. *J Biomech Eng-T Asme* 2000; **122**(6):630–639.
14. Zdero R, Bougherara H, Dubov A, Shah S, Zalzal P, Mahfud A *et al*. The effect of cortex thickness on intact femur biomechanics: a comparison of finite element analysis with synthetic femurs. *Proc Inst Mech Eng H* 2010;224(7):831–840.
15. Dragomir-Daescu D, Op Den Buijs J, McEligot S, Dai Y, Entwistle RC, Salas C *et al*. Robust QCT/FEA models of proximal femur stiffness and fracture load during a sideways fall on the hip. *Ann Biomed Eng* 2011;**39**(2):742–755.
16. Maehara Y, Tsujitani S, Saeki H, Oki E, Yoshinaga K, Emi Y *et al*. Biological mechanism and clinical effect of protein-bound polysaccharide K (KRESTIN): review of development and future perspectives. *Surg Today* 2012;**42**:8–28.
17. Harp JH, Aronson J, Hollis M. Noninvasive determination of bone stiffness for distraction osteogenesis by quantitative computed tomography scans. *Clin Orthop Relat Res* 1994; **301**(4):42–48.
18. Zhang B, Luo S, Wu B, Qiu P, Dai M. A new anterolateral approach for type C fractures of the distal femur. *Int Surg* 2014; **99**(6):875–879.